Bol. Soc. Paran. Mat. (3s.) **v. 37** 1 (2019): 99–111.
©SPM –ISSN-2175-1188 on line ISSN-00378712 in press
SPM: www.spm.uem.br/bspm doi:10.5269/bspm.v37i1.31396

Numerical Investigation of Nanofluid Turbulent Flow in a Wavy Channel With Different Wavelengths, Amplitudes & Phase Lag

Tooran Tavangar, Abbas Ramiar, Amir Arya, Reza Mohammadyari, Mazaher Rahimi-Esbo

abstract: Two dimensional incompressible turbulent nanofluid flow in a sinusoidal wavy channel is numerically investigated. Finite volume method and Rhie and Chow interpolation in a collocated grid arrangement are used for solving governing equations. The effects of the volume fraction of nanoparticles, Reynolds number, phase lag, frequency and amplitude of the wavy walls on the heat transfer rate are studied. The present work is shown good agreement with existing experimental and numerical results. Increasing the frequency and amplitude of the wave and nanoparticles volume fraction are the most important factor for changing heat transfer rate.

Key Words: Wavy channel; Nanofluid flow; Nusselt number; Phase lag.

Contents

Changing the fluid properties and flow geometry are two common ways of making an improvement in heat transfer rate. Using porous media, micro scale channels, increasing the surface and put a shackle in the way of the fluid are some methods for increasing heat transfer with changing the geometry. Adding nanoparticles to base fluid and using fluids with better properties are the ways for increasing heat transfer.

2010 *Mathematics Subject Classification:* 76F35, 76R50.
Submitted March 22, 2016. Published May 03, 2016

1. Nomenclature

c_p	specific heat (kJ/kg.K)
d	diameter (m)
d_p	average diameter of nanoparticles (m)
h	average height of the channel (m)
k	thermal conductivity (W/m.K)
k_b	Boltzmann number (J/K)
L	length of the channel (m)
$\dot{m}$	mass flow rate (kg/s)
$\hat{n}$	vector normal to the surface
Nu	Nusselt number
P	pressure (Pa)
Pr	Prandtl number
$\dot{Q}$	heat energy rate (J/s)
Re	Reynolds number
T	temperature (K)
u	x component of the velocity (m/s)
v	y component of the velocity (m/s)
V_b	Brownian velocity of nanoparticles (m/s)

2. Greek symbols

α_f	thermal diffusivity (m^2/s)
α	amplitude of the waves (m)
ϕ	volume fraction of nanoparticles
λ	wavelength (m)
μ	viscosity (Pa.s)
υ	kinematic viscosity (m^2/s)
ρ	density (kg/m^3)
$\overline{\sigma}$	length of curve (m)
δ	center to center distance of nanoparticles (m)

3. Subscripts

F	base fluid
Nf	Nanofluid
P	Particle
W	Wall

4. Introduction

Many researchers have focused on mentioned subjects. Choi et al. [1] applied large eddy simulation (LES) to simulate thermal fields of a turbulent flow in a wavy channel with various amplitudes. They showed that Both C_f and Nusslet number have the maximum value in the upper part of the wavy wall. Wall bending is found to effectively enhance the heat transfer. Another large eddy simulation (LES) is applied by Pham et al. [2] who studied turbulent flow in a wavy wall channel. They have used Colburn and Fanning factor for their analysis. Their work contains data for Reynolds numbers from 750 to 4500. Rostamiani et al. [3] numerically analyzed the turbulent nanofluid flow with different volume concentrations of nanoparticles through a two-dimensional duct under constant heat flux condition. They founded that by increasing the volume concentration, the wall shear stress and heat transfer rates increase. Also they reported for a constant volume concentration and Reynolds number, the effect of CuO nanoparticles yield to more enhancement in the Nusselt number and friction coefficient than Al_2O_3 and TiO_2 nanoparticles. Nassan et al. [4] experimentally compared heat transfer characteristics of Al_2O_3-water and CuO-water nanofluids through a square cross-section cupric duct in laminar flow under uniform heat flux condition. Their results indicate that a considerable heat transfer enhancement has been achieved by both nanofluids compared to the base fluid. However, CuO.water nanofluid showed more heat transfer augmentation compared with Al_2O_3-water nanofluid through square cross-section duct. Bianco et al. [5] numerically analyzed turbulent forced convection flow of water-Al_2O_3 nanofluid in a tube subjected to a constant and uniform temperature at the wall. The two-phase mixture model was employed to simulate the nanofluid convection, taking into account appropriate thermo physical properties. They founded that heat transfer enhancement is increasing with the particle volume concentration and Reynolds number. Ghaffari et al. [6] numerically investigated turbulent mixed convection of nanofluid consisting water and Al_2O_3 through a horizontal curved tube. They implemented two-phase mixture model to study such a flow field. They reported that the nanoparticles volume fraction does not have a direct effect on the secondary flow and the skin friction coefficient. However its effects on the thermal parameters and turbulent intensity are significant. A direct numerical simulation (DNS) was performed by Yoon et al. [7] in a channel with sinusoidal curved walls. Their research performed for various ratios of wave amplitudes to wave length $0.01 \leq \alpha/\lambda \leq 0.05$ and Reynolds number based on bulk velocity (U_b) was equal to 6760. They focused on observation of the fluid instead of heat transfer.

Although some researchers investigated the flow in a wavy channel, but none of them investigated the nanofluid flow in a wavy channel with phase lag. For the first time two dimensional steady turbulent flow of nanofluid in a sinusoidal curved wall channel have been numerically simulated. Suspension of water and nanoparticles of aluminum dioxide (AL_2O_3) have been used for this purpose. Effect of Reynolds numbers, wave amplitudes, wave lengths and phase lags is studied. In this paper a wide range of Reynolds numbers, from 3×10^3 to 10^5, wave amplitude changes from 0 m to 0.3 and wave length changes from 1 m to 24 has been investigated.

5. Physics of the problem and governing equations

Geometry of the problem is a channel with two direct sections at the entrance and exit. Wavy walls are at the middle part as shown in Fig. 1.

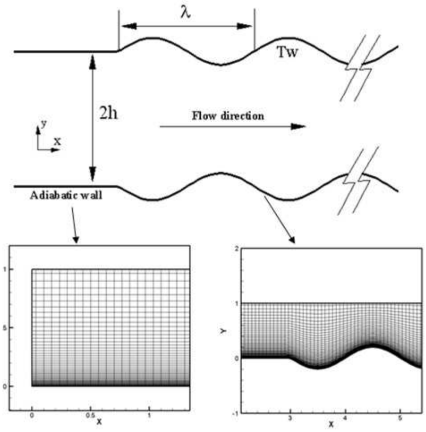

Figure 1: (a) Physical model, (b) Sample of grids used in present computing

The fluid enters the channel from left side and exits from the right side. The wavy walls in the top and bottom are considered isothermal and two direct sections of the channel at the top and bottom are considered as adiabatic walls. Amplitude, Reynolds number, phase lag and wavelength of the waves are parameters of the problem. The characteristic length for calculating Reynolds is h, which is average height of wavy walls. Function of wall is simple sinusoidal function of amplitude and wavelength. Maximum length for all cases is 20 m to guarantee the outflow boundary condition.
The continuity, momentum and energy equation for the 2D flow problem are given by:
1. Continuity:

$$\frac{\partial}{\partial x_i}(\rho_{nf} u_i) = 0 \tag{5.1}$$

2. Momentum:

$$\frac{\partial}{\partial x_j}(\rho_{nf} u_i u_j) = -\partial p/\partial x_i + \frac{\partial}{\partial x_j}\left[\mu(\partial u_i/\partial x_j + \partial u_j/\partial x_i)\right] + \frac{\partial}{\partial x_j}(-\rho_{nf}\overline{u_i' u_j'}) \tag{5.2}$$

3. Energy:

$$\frac{\partial}{\partial x_i}(\rho_{nf} u_i T) = \frac{\partial}{\partial x_j}((\Gamma + \Gamma_t)\frac{\partial T}{\partial x_j}) \tag{5.3}$$

Where Γ and Γ_t are the molecular thermal diffusivity and turbulent thermal diffusivity, respectively and are given by:

$$\Gamma = \mu_{nf}/\mathrm{Pr}_{nf} \quad , \qquad \Gamma_t = \mu_t/\mathrm{Pr}_t \tag{5.4}$$

The Reynolds-averaged approach for turbulence modeling requires that the Reynolds stresses, i.e. $\rho_{nf}\overline{u_i'\,u_j'}$ needs to be modeled. For this purpose $k-\varepsilon$ model is chosen. A common method employs the Boussinesq hypothesis to relate the Reynolds stresses to the mean velocity gradients:

$$\rho_{nf}\overline{u_i'\,u_j'} = \mu_t(\partial u_i/\partial x_j + \partial u_j/\partial x_i) \tag{5.5}$$

The turbulent viscosity term is to be computed. It is defined as below equation:

$$\mu_t = \rho_{nf} c_\mu\, k^2/\varepsilon \tag{5.6}$$

4. Transport equation for k and ε

$$\frac{\partial}{\partial x_i}(\rho_{nf} k u_i) = \frac{\partial}{\partial x_j}\left[\left(\mu_{nf} + \frac{\mu_t}{\sigma_k}\right)\frac{\partial k}{\partial x_j}\right] + G_k - \rho_{nf}\varepsilon + S_k \tag{5.7}$$

and

$$\frac{\partial}{\partial x_i}(\rho_{nf} \varepsilon u_i) = \frac{\partial}{\partial x_j}\left[\left(\mu_{nf} + \frac{\mu_t}{\sigma_\varepsilon}\right)\frac{\partial \varepsilon}{\partial x_j}\right] + C_{1\varepsilon}\frac{\varepsilon}{k}G_k + C_{2\varepsilon}\rho_{nf}\frac{\varepsilon^2}{k} + S_\varepsilon \tag{5.8}$$

G_k is the rate of turbulent kinetic energy generation and $\rho\varepsilon$ is its destruction rate, and is written as:

$$G_k = -\rho_{nf}\overline{u_i'\,u_j'}\frac{\partial\, u_j}{\partial x_i} \tag{5.9}$$

s_k and s_ε are source term for k and ε and in this research are taken as zero. The boundary values for the turbulent quantities near the wall are specified with the standard wall-treatment method. The values of $C_\mu = 0.009$, $C_{1\varepsilon} = 1.44$, $C_{2\varepsilon} = 1.92$, $\sigma_k = 1$, $\sigma_\varepsilon = 1.3$ and $\mathrm{Pr}_t = 0.9$ are chosen to be the empirical constants in the turbulence transport equations [?]. Below equation are used to calculate the turbulent intensity (I), turbulent kinetic energy (k) and turbulent dissipation rate (ε) at the inlet section of the channel.

$$\begin{aligned} &I = 0.16\ \mathrm{Re}^{-1/8} \\ &k = (3/2)(I \times u_{in})^2 \\ &\varepsilon = c_\mu^{0.75} \times (k^{1.5}/0.1h) \end{aligned} \tag{5.10}$$

For obtaining thermo physical properties, there are different approaches available. These approaches can be categorized by how they treat with nanoparticles and fluid interaction. Homogenous nanofluid is a common method. Homogenous nanofluid is a common method that nanoparticles and fluid are assumed to be in thermal equilibrium and nanoparticles velocity is as the same as fluid velocity. So there is no slip between nanoparticles and the fluid.

The thermal conductivity of the nanofluid is calculated from Chon et al [8], which is expressed in the following form:

$$\frac{K_{nf}}{K_f} = 1 + 64.7\,\phi^{0.746}(d_f/d_p)^{0.369} \times\ (K_p/K_f)^{0.7476}\,\mathrm{Pr}_f^{0.9955}\,\mathrm{Re}_p^{1.2321} \tag{5.11}$$

where:

$$\mathrm{Pr}_f = \mu_f/\rho_f\alpha_f \tag{5.12}$$

$$\mathrm{Re}_p = \rho_f K_b T/3\,\pi\,\mu^2 l_f \tag{5.13}$$

$$\mathrm{d_p} = 36 \times 10^{-9}\,(m) \tag{5.14}$$

Pr_f, Re_p and d_p are Prandtl number, Reynolds number and mean diameter of nanoparticles respectively.

k_b is the Boltzmann constant, 1.3807×10^{-23} and l_f is the free average distance of water molecules that according to Chon and et al's suggestion is taken to 17 nm. Minsta et al. [9] approved the accuracy of this model.

The viscosity of the nanofluid is approximated as viscosity of the base fluid $\mu_\mathrm{f}$containing dilute suspension of fine spherical particles as given by Masoumi et al [10]:

$$\frac{\mu_{nf}}{\mu_f} = 1 + \rho_p\,V_b\,d_p^2/72\,N\,\delta \tag{5.15}$$

where:

$$\delta = \sqrt[3]{\pi/6\,\phi} \times d_p$$

$$V_b = (1/d_p)\sqrt{18\,k_b T/\pi\ \_\rho_p\,d_p}$$

δ is the mean center to center distance of nanoparticles and V_b Brownian velocity of nanoparticles. $N = (c_1\phi + c_2)\,d_p + (c_3\phi + c_4)$ is a parameter for adapting the results with experimental data where $c_1 = -1.133 \times 10^{-6}, c_2 = -2.771\ \times 10^{-6}$, $c_3 = 9.0 \times 10^{-8}$ and $c_4 = -3.93 \times 10^{-7}$.

The density and specific heat of the nanofluid are calculated by using the Pak and Cho [11] correlations, which are defined as follows:

$$\rho_{nf} = \phi\,\rho_p + (1-\phi)\,\rho_f \tag{5.16}$$

$$(c_p)_{nf}\!= ((1\!-\!\phi) \times \rho_f \times (c_p)_f + \phi \times (\rho \times c_p)_\mathrm{p})/\rho_{nf} \tag{5.17}$$

$$\mathrm{Pr_{nf}}\!=\!\mu_\mathrm{nf} \times c_{\mathrm{p_{nf}}}/\,K_\mathrm{nf} \tag{5.18}$$

For inlet and outlet of the channel, and for isothermal and adiabatic walls, boundary conditions can be expressed like below:

$$\frac{\partial T}{\partial x} = 0,\ \frac{\partial u}{\partial x} = 0 \text{ for outflow boundary condition} \tag{5.19}$$

$$T = T_w,\ u = v = 0 \text{ for isothermal boundary conditions} \tag{5.20}$$

$$\frac{\partial T}{\partial \hat{n}} = 0,\ u = v = 0 \text{ for adiabatic boundary conditions} \tag{5.21}$$

The Reynolds number is defined as:

$$\mathrm{Re} = \frac{\rho_f U_{in} h}{\mu_f}. \tag{5.22}$$

Local Nusselt number can be defined as:

$$Nu_x = -\frac{k_{nf}}{k_f} \frac{h\,(\partial T/\partial \hat{n})}{T_{in} - T_y}\bigg|_{y=s(x)}, \tag{5.23}$$

While $\frac{\partial T}{\partial \hat{n}}$ is the temperature gradient normal to the walls.

$$\frac{\partial T}{\partial \hat{n}} = \vec{\nabla} T.\hat{n} \tag{5.24}$$

$\overline{Nu}$ is the average Nusselt number.

$$\overline{Nu} = \frac{\dot{Q} L}{A k_f \Delta T} \frac{\overline{\sigma}}{\overline{x}}, \tag{5.25}$$

Where $\dot{Q}$ is the total heat transfer rate through the channel and $\bar{\sigma}$ is the length of the curve and can be calculated as:

$$\overline{\sigma} = \int_{x_s}^{x} \left(1 + \left(\frac{\partial y}{\partial x}\right)^2\right)^{1/2} \tag{5.26}$$

$\dot{Q}$ is the total heat transfer rate.

$$\dot{Q} = \dot{m} c_f (T_{bulk} - T_w)\,|_{x=L} \tag{5.27}$$

where T_{bulk} is the mean temperature and can be calculated as defined below:

$$T_{bulk} = \frac{\int_{A_c} \rho u c_v T dA_c}{\dot{m} c_v} \tag{5.28}$$

6. Results and discussion

For mesh independency, the results of several meshes (250×70, 300×80, 350×90, 450×130, 450×150, 500×150, and 500×170) have been compared. It can be seen from Fig. 2 that 500×150 nodes is enough to achieve accurate results.

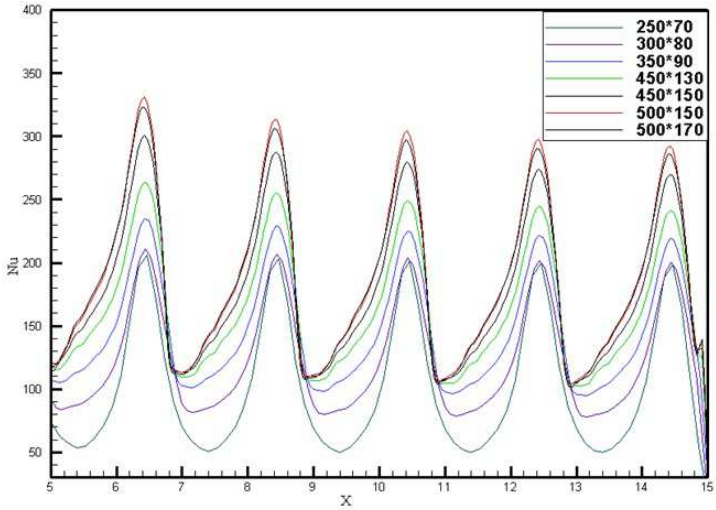

Figure 2: Results for different grids $\mathrm{Re} = 2 \times 10^3$, $\alpha = 0.2$, $\phi = 0$ and $\lambda = 2$.

The present results are compared with experimental data of Zhang et al. [1] and numerical results of Pham et al. [2]. They have used Colburn factor for their analysis. They investigated the effect of Reynolds numbers from 750 to 4500. As it can be seen from Fig. 3 there is an acceptable agreement between their result and current study.

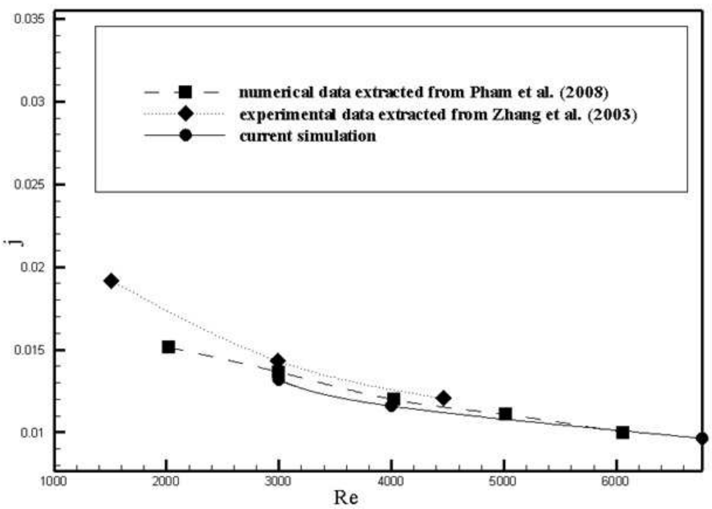

Figure 3: Comparison of present work with available data

Present calculation was performed for $\mathrm{Re} = 4000$ to $\mathrm{Re} = 100,000$, $\mathrm{Pr} = 6.5$,

$\alpha = 0.0$ to 0.3, $\phi = 0.0$ to 0.05, and $\lambda = 1$ to 12 meters. The fluid considered is a suspension of $\phi = 0.0$ to 0.05, Al_2O_3 nanoparticles in water. Figure 4. shows the particle volume concentration and flow Reynolds number effect on the average Nusselt number. It can be seen that the average Nusselt number increases with an increase in the nanoparticles volume concentration as well as an increase in the flow Reynolds number. The figure reveals an enhancement in average Nusselt number by increasing the volume fraction of nanoparticles. This behavior can be inferred from Eq. . The effect of nanoparticles on the temperature difference term is negligible. The effect of volume fraction of nanoparticles on the temperature gradient term and on the thermal conductivity ratio term is more pronounced. The equations show that any increase in volume fraction increases inertia forces because ρ_{nf} will be increased and accordingly increases the temperature gradient. Besides, the nanoparticles increase the thermal conductivity ratio term as it can be seen from Eq. . Therefore, both the temperature gradient term and thermal conductivity ratio term increase by increasing the volume fraction of nanoparticles. Accordingly, It can be seen that by increasing volume fraction the Nusselt number will be increased, because the heat transfer properties is improved.

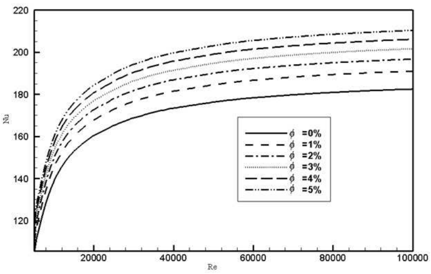

Figure 4: Average Nusselt number for different Reynolds and different volume fractions $\lambda = 2$ and $\alpha = 0.2$.

The effect of amplitude on Nusselt number is depicted in Fig. 5.

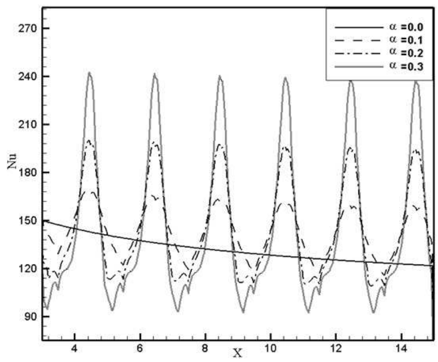

(a)

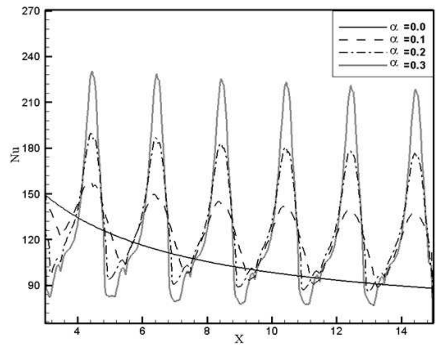

(b)

Figure 5: Local Nusselt number for different wave amplitudes, $\phi = 0$ and $\lambda = 2$ (a) $\mathrm{Re} = 2 \times 10^4$ (b) $\mathrm{Re} = 6 \times 10^4$.

By increasing amplitude flow cannot follow the body so it will separates from it. This separations form recirculation zones in the dip of the wall. This recirculation zones prevent the cold fluid to contact with hot wall, so they decrease local Nusselt number. Figure 6 shows these recirculation zones using velocity vectors. On the other hand increasing the wave amplitudes will increase the chaotic behavior of the fluid flow which leads to be more impact between molecules of the fluid and the walls. These impacts cause more energy absorption by the fluid along the channel. These cause an average Nusselt number increase on both top and bottom walls.

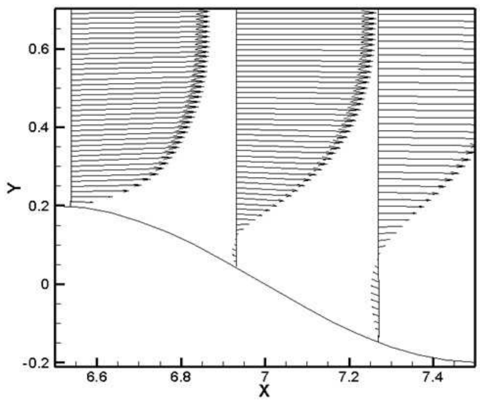

Figure 6: Velocity vectors in different sections $\mathrm{Re} = 2 \times 10^4$, $\alpha = 0.2$ and $\lambda = 2$.

Different phase lags will change the behavior of the fluid and it can be used in an order to weaken the recirculation zones. In Fig. 7 the effect of phase lag on heat transfer is shown. A high heat transfer enhancement is observed for 135 and 225 phase lag degrees.

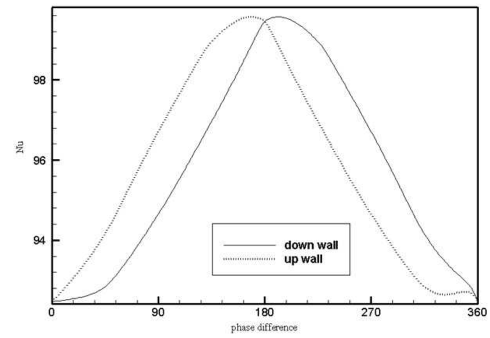

Figure 7: Average Nusselt number. Re $= 6 \times 10^4$, $\phi = 0$, $\alpha = 0.2$ and $\lambda = 2$.

Another parameter which is important in heat transfer enhancement is the wavelength of the wavy walls. Figure 8. shows average Nusselt number in different wavelengths.

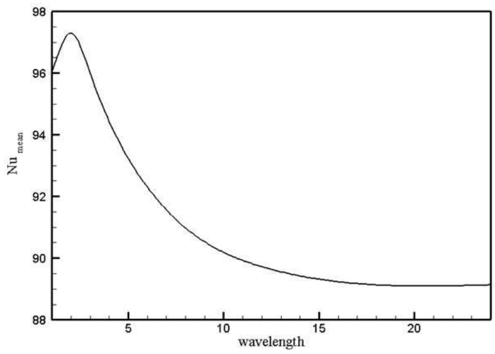

(a)

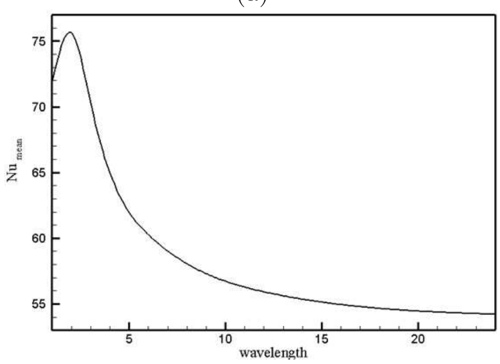

(b)

Figure 8: Average Nusselt number for $\phi = 0$ and $\alpha = 0.2$ (a) Re $= 10^4$ (b) Re $= 6 \times 10^4$.

As it can be seen in these figure average Nusselt number takes a pick with reducing wavelength. The enhancement of average Nusselt number for greater wavelengths is a result of enhancement of the contact surface. But as it was debated before recirculation zones have a negative effect on heat transfer. The reduction of average Nusselt number in lower wavelengths can be justified with recirculation zone effect. In lower wavelengths, these recirculation zones will become stronger and will lead to heat transfer reduction.

7. Conclusion

Forced convection of a turbulent flow in a wavy wall channel has been numerically studied. The results show that by increasing the Reynolds number, aspect ratio and amplitude the average Nusselt number will increase. Also the effects of different phase and different wavelengths of the wavy walls have been investigated. The results reveal that by enhancement of aspect ratio, the penetration of the jet flow in the duct and the developing length increases simultaneously. Also, this effect can is seen by increasing the Reynolds number. Furthermore it was demonstrated in the investigations that by increasing the Reynolds number and aspect ratio, the length of the recirculation zones raises and as a result affects on the local Nusselt number and consequently the average Nusselt number.

References

1. Choi, S.U.S., 1995, "Enhancing thermal conductivity of fluids with nanoparticles in developments and applications of non-Newtonian flows," ASME FED 231/ MD 66, pp. 99–103.

2. Pham, M.V., Plourde, F. S., Doan, K., 2008, "Turbulent heat and mass transfer in sinusoidal wavy channels," International Journal of Heat and Fluid Flow 29, pp. 1240- 1257.

3. Rostamani, M., Hosseinizadeh, S.F., Gorji, M. and Khodadadi, J.M., 2010, "Numerical study of turbulent forced convection flow of nanofluids in a long horizontal duct considering variable properties," International Communication in Heat and Mass Transfer 37, pp. 1426-1431.

4. Nassan, H. T., Heris, S. Z., and Noie, S.H., 2010, "A comparison of experimental heat transfer characteristics for Al_2O_3-water and CuO-water nanofluids in square cross-section duct," International Comminucation in Heat and Mass Transfer, 37, pp. 924-928.

5. Bianco, V. , Manca, O., and S. Nardini, 2010, "Numerical simulation of water/Al_2O_3 Nanofluid turbulent Convection," Advances in Mechanical Engineering, pp. 1-10.

6. Ghaffari, O., Behzadmehr, A. and H. Ajam, 2010, "Turbulent mixed convection of a nanofluid in a horizontal curved tube using a two-phase approach," International Communication in Heat and Mass Transfer 37, pp. 1555-1558.

7. Yoon, H.S., El-Samni, O.A., Huynh, A.T., Chun, H.H., Kim, H.J., Pham, A.H., and Park, I.R., 2009, "Effect of wave amplitude on turbulent flow in a wavy channel by direct numerical simulation," Ocean Engineering journal, 36, pp. 697–707.

8. Chon, C.H., Kihm, K.D., Lee, S.P. and Choi, S. U. S., 2005, "Empirical correlation finding the role of temperature and particle size for nanofluid (Al_2O_3), Thermal conductivity enhancement," Applied Physics Letters 87, pp. 153107–153110.

9. Mintsa, H.A., Roy, G., Nguyen, C.T. and Doucet, D., 2009, "New temperature dependent thermal conductivity data for water-based nanofluids," International Journal of Thermal Sciences 48, pp. 363–371.

10. Masoumi, N., Sohrabi, N. and Behzadmehr, A.A., 2009, "New model for calculating the effective viscosity of nanofluids," Journal of Physics D: Applied Physics 42, pp. 055501-055506.

11. Pak, B.C. and Cho, Y.I., 1998, "Hydrodynamic and heat transfer study of dispersed fluids with submicron metallic oxide particles," Experimental Heat Transfer 11, pp. 151–170.

12. Zhang, J., Muley, A., Borghese, J.B., Manglik, R.M., 2003, "Computational and experimental study of enhanced laminar flow heat transfer in three dimensional sinusoidal wavy-plate-fin channels," ASME Summer Heat Transfer Conference, Las Vegas, NV, July pp. 21–23.

Tooran Tavangar,
Department of Mechanical Engineering,
Amirkabir University of Technology, 424,
Hafez Ave., 15875-4413 Tehran, Iran.

and

Abbas Ramiar,
Amir Arya,
Faculty of Mechanical Engineering,
Babol University of Technology,
POB 484, Babol, Iran.

and

Reza Mohammadyari,
Mazaher Rahimi-Esbo,
Department of Mathematics,
Buinzahra Branch, Islamic Azad University,
Buinzahra, Iran.
E-mail address: Rahimi.mazaher@gmail.com - Tel/Fax: +98(911) 6277073